Computers and Mathematics with Applications 60 (2010) 3108–3122

Contents lists available at ScienceDirect

Computers and Mathematics with Applications

journal homepage: www.elsevier.com/locate/camwa

Six strategies for defeating the Runge Phenomenon in Gaussian radial basis functions on a finite interval☆

John P. Boyd

Department of Atmospheric, Oceanic and Space Science, University of Michigan, 2455 Hayward Avenue, Ann Arbor MI 48109, United States

ARTICLE INFO

Article history:
Received 19 August 2010
Accepted 5 October 2010

Keywords:
Radial basis function
Runge Phenomenon

ABSTRACT

Radial basis function (RBF) interpolation is a "meshless" strategy with great promise for adaptive approximation. Because it is meshless, there is no canonical grid to act as a starting point for function-adaptive grid modification. Uniform grids are therefore common with RBFs. Like polynomial interpolation, which is the limit of RBF interpolation when the RBF functions are very wide (the "flat limit"), RBF interpolants are vulnerable to the Runge Phenomenon, whether the grid is uniform or irregular: the N-point interpolant may *diverge* as $N \to \infty$ on the interval spanned by the interpolation points even for a function $f(x)$ that is analytic everywhere on and near this interval.

In this work, we discuss six strategies for defeating the Runge Phenomenon, specializing to a *uniform* grid on a finite interval and one particular species of RBFs in one space dimension: $\phi(x) = \exp(-[\alpha^2/h^2]x^2)$ where h is the grid spacing. Three strategies fail, but three are successful. One good strategy is to vary α with the number of interpolation points N as $N^{-1/4}$. Unfortunately this gives both a subgeometric rate of convergence for the approximation (error falling as $\exp(-q\sqrt{N})$ for some constant q) and a matrix condition number that grows as $\exp(p\sqrt{N})$ for some $p > 0$. (In order to explain why *fixed* α, independent of N, is not a convergent strategy, we digress to discuss error saturation, and show experimentally that the saturation error on the finite interval is about $0.6\exp(-0.47/\alpha^2)\|f\|_\infty$; if a user-chosen error tolerance δ is acceptable, then the optimum choice is $\alpha_{optimum}(\delta) = 1/\sqrt{-2\log(\delta/0.06)}$.) The second good strategy is RBF Extension, which uses RBF functions with centers on a interval slightly larger than the target interval to approximate $f(x)$. A third strategy is to split the interval into two "boundary layers" and a large middle interval and apply separate RBF approximations on each. The slow-decrease-of-α strategy is much cheaper, but RBF Extension is much more resistant to ill-conditioning and therefore can achieve much lower errors. The three-interval method is the least accurate, but is robust and inexpensive.

1. Introduction

Radial basis functions have become an important weapon in computer graphics and adaptive numerical solutions to differential equations [1–8]. The RBF approximation to a function in any number of dimensions d is

$$f(\vec{x}) \approx \sum_{j=1}^{N} \lambda_j \phi\left(\|\vec{x} - \vec{c}_j\|_2\right) \quad \vec{x} \in R^d \tag{1}$$

☆ This work was supported by NSF grant OCE0451951.
E-mail address: jpboyd@umich.edu.

0898-1221/$ – see front matter © 2010 Elsevier Ltd. All rights reserved.
doi:10.1016/j.camwa.2010.10.015

for some function $\phi(r)$ and some set of N points $\vec{c}_j$, which are called the "centers". The coefficients λ_j are usually found by interpolation at a set of points $\vec{x}_k$ that may or may not coincide with the centers. In the rest of this article, we shall concentrate on the one-dimensional case, $d = 1$, and assume the centers and interpolation points coincide, that is, $\vec{c}_j = \vec{x}_j$.

Like polynomials, RBFs on a finite interval exhibit the Runge Phenomenon.

Definition 1 (*Runge Phenomenon*)**.** Let $f_N(x)$ denote the N-point interpolant of some function $f(x)$ using some basis, here radial basis functions, with the interpolation points spanning an interval which without loss of generality can always be normalized to $x \in [-1, 1]$. The Runge Phenomenon is the divergence of the interpolant $f_N(x)$ as $N \to \infty$ for some $f(x)$ that are analytic everywhere on and near the interval $x \in [-1, 1]$. This will happen if $f(x)$, the function being approximated, has singularities anywhere within a certain grid-dependent and basis-dependent domain in the complex plane known as the "Runge Zone" [9].

For finite N, the Runge Phenomenon manifests itself as wild, increasing-with-N oscillations *between* the interpolation points. (At the interpolant points themselves, of course, $f_N(x_j) = f(x_j)$ by construction.) For polynomial interpolation on a uniform grid, the oscillations are localized near $x = \pm 1$, but other grids and other basis functions may yield Runge oscillations anywhere within the interval as illustrated well in [10]. When the Runge Zone is not known analytically, as true of RBFs except for the special case of [9], it can be computed numerically [11].

In previous articles, we have described a plenitude of strategies for defeating the Runge Phenomenon in *polynomials* [12–15]. Here, we do the same for radial basis functions.

Although many types of $\phi(r)$ have been used in the literature as reviewed in [16], we prefer to forgo a catalogue of shallow results in favor of an in-depth examination of a single important case: that of Gaussian RBFs for which

$$\phi(x) \equiv \exp(-\epsilon^2 x^2). \tag{2}$$

In other work [17–20], we have treated the one-dimensional domain without boundaries. Here, we focus on the complications that arise when the domain is restricted to a finite interval which we shall standardize to $x \in [-1, 1]$ without loss of generality. (A general interval $y \in [a, b]$ can always be mapped into the canonical interval by $y = (a + b)/2 + (b - a)x/2$.)

One notational complication is that there are actually three different but useful ways of measuring the width of the RBFs:

Definition 2 (*Gaussian RBF Width Parameters*)**.** With $N + 1$ interpolation points on $x \in [-1, 1]$ and denoting the grid spacing by h ($= 2/N$ for a uniform grid, or defining it as the *average* grid spacing if the grid is not uniform), the RBF basis functions may be written equivalently as

$$\phi(x) = \exp(-\epsilon^2 x^2) \tag{3}$$

$$= \exp(-(\beta/4)Nx^2) \tag{4}$$

$$= \exp(-\alpha^2 (x/h)^2) \tag{5}$$

where

1. ϵ is the ABSOLUTE width parameter
2. β is the RUNGE/GEOMETRIC width parameter
3. α is the RELATIVE width parameter.

(Note that strictly these are all *inverse* width parameters in the sense that the RBF $\phi(x)$ is narrow when ϵ is large.) The interrelationships are

$$\epsilon = \frac{1}{2}\sqrt{N}\sqrt{\beta} = \frac{N}{2}\alpha; \quad \alpha = \frac{2}{N}\epsilon = \sqrt{\frac{\beta}{N}}; \ \beta = N\alpha^2 = 4\frac{\epsilon^2}{N}. \tag{6}$$

The "Runge/geometric" parameter β is so named because this variation of width-with-N is necessary to obtain a geometric rate of convergence as explained further below. β also controls the size of the Runge Zone $\mathcal{D}(\beta)$ in the complex x-plane as illustrated in [9]. The "relative" width parameter α is the width *relative* to the average *grid spacing* h: for fixed α, the e-folding scale in units of h is independent of N. For this reason, the fixed-α approximation is dubbed the "stationary approximation" in Fasshauer [21]. The absolute inverse width ϵ is widely used in the literature but not here.

One major limitation of the present work is that it is non-adaptive. Function-adaptive methods, which tailor the grid to the function, are obviously another strategy for defeating the Runge Phenomenon. Successful experiments are reported in [22,10]. However, it is hardly a secret that adaptive methods, not just for radial basis functions but for finite difference, finite element and finite volume algorithms, too, are a subject of intense research despite many successes. Adaptive methods need a solid foundation in non-adaptive strategies, and that is what we aim to provide here.

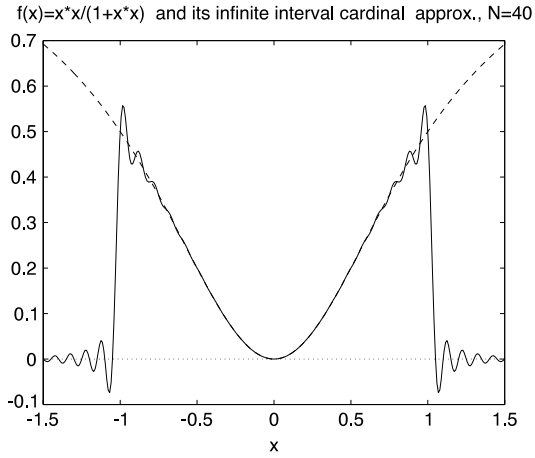

Fig. 1. A comparison of $f(x) = x^2/(1+x^2)$ [dashed] with its approximation by 41 infinite interval cardinal functions ($\alpha = 1/2$) with a grid spacing of $h = 1/20$ [solid]. The cardinal function series converges to $\hat{f}$, which is $f(x)$ multiplied by the characteristic function of the interval $[-1, 1]$. The oscillations at the discontinuities of $\hat{f}$ are the spoor of Gibbs Phenomenon.

2. Three failed attempts to defeat the Runge Phenomenon

2.1. Truncated infinite interval approximation: fails

Any reasonable basis can be rearranged into a "cardinal" or "Lagrange basis" $C_j(x)$ such that

$$C_j(x_k) = \begin{cases} 1, & j = k \\ 0, & j \neq k. \end{cases} \tag{7}$$

Boyd and Wang [18] show that the cardinal functions for Gaussian RBFs on the *infinite* interval are given by

$$C_j^{\text{infin}}(x; h, \alpha) = C(x/h - j; \alpha) \tag{8}$$

$$C(X; \alpha) \approx \frac{\alpha^2}{\pi} \frac{\sin(\pi X)}{\sinh(\alpha^2 X)} \left\{1 + O\left(4\exp(-2\pi^2/\alpha^2)\right)\right\}. \tag{9}$$

Because the infinite interval cardinal functions never blow up and are always well-behaved, it is tempting to defeat the Runge Phenomenon by substituting the infinite interval cardinal functions for the finite interval cardinal functions. However, this is equivalent to approximating $f(x)$ on the infinite interval by

$$f(x) \approx \hat{f}(x) \equiv \begin{cases} f(x), & x \in [-1, 1] \\ 0, & |x| > 1. \end{cases} \tag{10}$$

That is to say, approximating $f(x)$ by ignoring the infinite interval cardinal functions associated with $|x| > 1$. Because of the discontinuity of $\hat{f}(x)$, the series of $C_j^{\text{infin}}(x; h)$ displays Gibbs Phenomenon and converges rather poorly as illustrated in Fig. 1.

2.2. Replacing interior finite interval cardinal functions with infinite interval cardinal functions: fails

An alternative strategy is to replace just the ill-behaved *interior* cardinal functions with infinite interval cardinal functions. However, Fig. 2 show that this strategy also fails: the errors are huge except for the last point on the left which is just the error for a standard finite interval approximation. (Note that for this particular $f(x)$, the singularities are well outside the Runge Zone, so the true finite interval cardinal functions, without substitution of infinite interval cardinal functions, converge.)

2.3. Blended approximations: fails

Another failed strategy is to introduce a window function $\mathcal{T}$ which is approximately equal to one on the center of the interval, zero for large $|x|$ and varies smoothly between these limits in a narrow transition layer; an explicit example is defined by (33). We then tried to blend infinite interval cardinal functions, $C_j^{\text{infin}}(x)$ with finite interval cardinal functions as

$$f(x) \approx \sum_j f(x_j) \left\{\mathcal{T}(x; w, \lambda) C_j^{\text{infin}}(x) + (1 - \mathcal{T}(x; w, \lambda))\, C_j(x)\right\}. \tag{11}$$

This was such a flop that we do not even bother to show a graph.

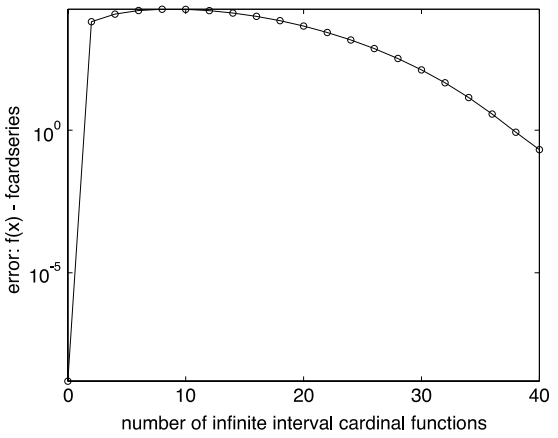

Fig. 2. Approximation of $f(x) = 1/(1 + x^2)$ by 41 cardinal functions when various numbers of finite interval RBF functions (horizontal axis) are replaced by infinite interval cardinal functions.

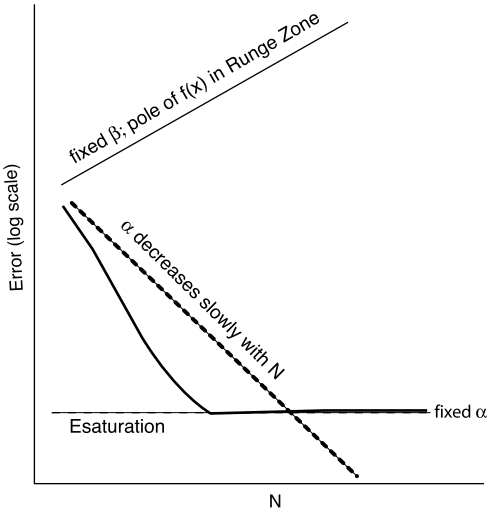

Fig. 3. Schematic of convergence of RBF interpolation in various limits, illustrated by plotting $\max_{x\in[-1,1]} |f(x) - f_N(x)|$ on a logarithmic scale versus N, the number of interpolation points.

The simple strategies unfortunately do not work. In this next three sections, we shall discuss three more intricate strategies which succeed.

3. Defeating the Runge Phenomenon by decreasing α as $1/N^{1/4}$

The way that the width parameters vary with N, the number of interpolation points, is crucial in what follows. As shown schematically in Fig. 3, when the *relative* width α is fixed, the error falls with increasing N up to a point and then levels off at a "saturation level". Error saturation is the theme of Section 4.

Platte and Driscoll have shown that when the Runge inverse width parameter β is fixed, the error either converges or diverges *geometrically*, that is, proportional to $\exp(-qN)$ for some constant q [9]. If $f(x)$ has a pole or other singularity within the Runge Zone $\mathcal{D}(\beta)$ in the complex x-plane, then the interpolation will diverge as illustrated in Fig. 3. If $f(x)$ has singularities (in the sense of complex variable theory) only outside the Runge Zone (not illustrated), then the interpolation will converge, also at a geometric rate, which again translates into a curve of asymptotically constant slope on a log-linear plot.

When the width-relative-to-the-grid-spacing parameter α is fixed, the error saturates, as already noted. However, the Runge Phenomenon seems to be missing in this limit. An obvious question is: what happens if the relative width parameter α decreases with N more slowly than the $1/\sqrt{N}$ proportionality when β is fixed?

The answer is: the Runge Phenomenon disappears and a subgeometric rate of convergence is achieved in the sense that the error falls as $\exp(-p\sqrt{N})$ rather than as a exponential *linear* in N as illustrated in Fig. 4. (The terminology is from [23].)

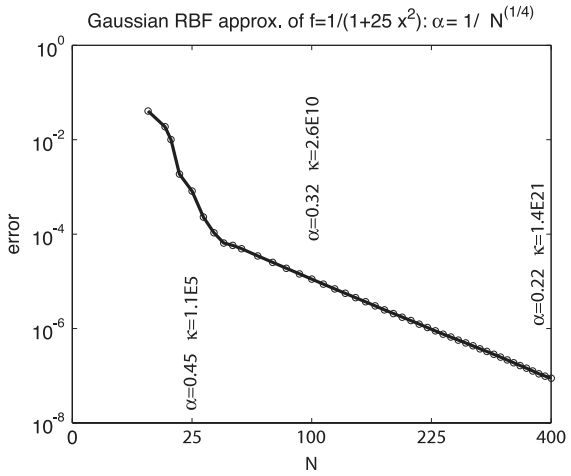

Fig. 4. Errors in the L_∞ norm for the Gaussian RBF approximation of $f(x) = 1/(1+25x^2)$, plotted versus $\sqrt{N}$. The relative width α varies with N as $N^{-1/4}$.

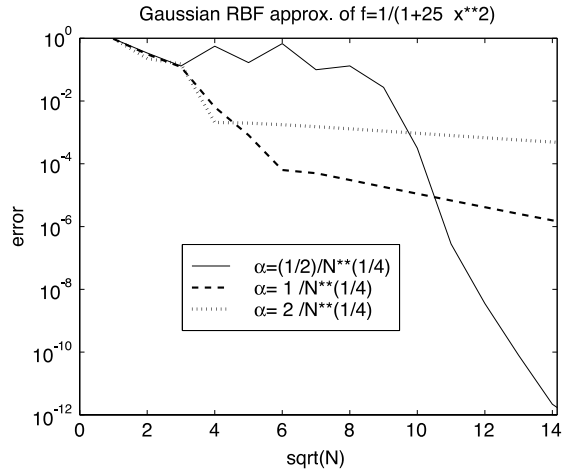

Fig. 5. Same as previous figure but for three different relationships between α and N.

Platte and Driscoll [9] have shown that Gaussian RBF interpolation on a uniform grid can be converted, through the change of coordinate $s = \exp(\beta x)$, to *polynomial* interpolation on a non-uniform grid on $s \in [\exp(-\beta), \exp(\beta)]$. They show that the Runge Zone $\mathcal{D}(\beta)$ becomes more and more tightly confined about the interval $x \in [-1, 1]$ as β increases, suggesting that the Runge Phenomenon is impossible in our strategy where $\beta \sim O(\sqrt{N})$ as $N \to \infty$. This argument falls short of a proof, however, because their work is the limit $N \to \infty$ for *fixed* β whereas the "α-decrease" strategy corresponds to the *simultaneous* limit that N and β tend to infinity *together*. A rigorous proof can probably be supplied along the lines of Section 3 of [15], but because of the length of that analysis, a formal proof is omitted here.

Unfortunately, as $N \to \infty$ in this limit intermediate between fixed α and fixed β, the condition number κ of the interpolation matrix is *exponentially increasing* as indicated by the vertical labels on the graph. This implies that it is increasingly difficult to accurately solve the matrix problem for the interpolant [24]. These computations were performed using multiprecision arithmetic in Maple because the condition number for $N = 400$ is much larger than the reciprocal of machine epsilon, implying that standard IEEE floating point arithmetic is useless.

Fig. 5 shows the effects of varying the constant ρ in the proportionality $\alpha = \rho/N^{1/4}$. The smallest α gives a slow rate of convergence for small N, but much better results for larger N.

Fig. 6 is a contour plot of error in the $N - \alpha$ plane for a different example, one with singularities much closer to the expansion interval. To avoid biases caused by singularities only near the endpoints or only near the middle of the interval, this $f(x)$ has poles near both $x = 0$ and $x = \pm 1$. The same general trend is seen as in the previous two figures: following the guideline $\alpha = N^{-1/4}$, we pass to deeper and deeper blue which implies convergence. However, if we fix β (lower guideline), the error *diverges* with increasing N, which is the Runge Phenomenon.

Two obvious questions arise. First, if decreasing α with N more slowly than in the fixed β limit is good, would it not be better still to keep α *fixed*? Second, accuracy is clearly sensitive to α: Is it possible to provide some guidance for choosing α?

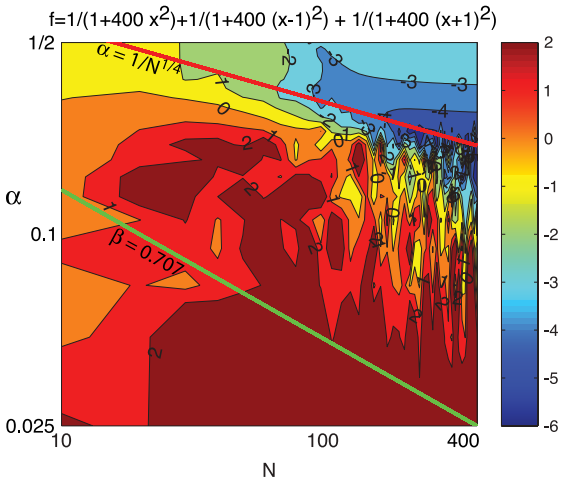

Fig. 6. Isolines of the base-10 logarithm of the error in the RBF approximation for $f(x) = 1/(1+400x^2) + 1/(1+400[x-1]^2) + 1/(1+400[x+1]^2)$ on $x \in [-1, 1]$. Logarithmic scales are used for both α and N so that power-law $\alpha(N)$ behavior appears as straight lines. The thick upper red line is $\alpha = N^{-1/4}$; this lies in a valley of decreasing error as N increases. Along the lower thick green line, $\beta = 1/\sqrt{2}$ ($\alpha = (1/2)N^{-1/2}$), the error DIVERGES. (For interpretation of the references to colour in this figure legend, the reader is referred to the web version of this article.)

The answer to both questions depend upon the "error saturation". We therefore digress from the discussion of the Runge Phenomenon to describe error saturation in the next section.

4. Error saturation

Definition 3 (*Error Saturation*)**.** When an RBF interpolant for fixed α, the "stationary limit" [21], does not converge to zero error, but only to a finite error $\mathcal{E}_{\text{saturation}}(\alpha)$, this lack of convergence to zero is called "error saturation".

"Error saturation" has been known for many years as reviewed in [21], going back to Buhmann's (1989) doctoral thesis.

Boyd and Wang [19] and, by a different route, Maz'ya and Schmidt [25], have shown that the saturation error for Gaussian RBFs on an infinite, uniform interval is

$$\mathcal{E}_{\text{saturation}}(\alpha) \equiv \lim_{N\to\infty} \|f(x) - f_{\text{RBF}}(x;\alpha,N)\|_\infty = 4\exp(-\pi^2/\alpha^2)\|f(x)\|_\infty. \tag{12}$$

Boyd and Bridge [26] show that on a *nonuniform* grid, the saturation error rises steeply to $O(\exp(-\pi^2/(4\alpha^2)))$; for example, on an otherwise uniform grid with one point missing,

$$\mathcal{E}_{\text{saturation}}(\alpha) \sim \frac{2\pi}{\alpha^2}\exp\left(-\frac{\pi^2}{4\alpha^2}\right)\|f(x)\|_\infty. \tag{13}$$

Boyd [27] shows that the saturation on a finite interval is larger still:

$$E_{\text{saturation}} \approx 0.058\exp(-0.467/\alpha^2)\|f(x)\|_\infty. \tag{14}$$

This empirical fit has the same form as for the infinite interval, both proportional to $\exp(-c/\alpha^2)$ for some constant c, but $c = \pi^2 \approx 10$ for the unbounded domain whereas $c \approx 0.467$, roughly twenty times smaller, for the finite domain. Unfortunately, this finite interval saturation is the case pertinent here.

5. An optimal choice of α

Small α (i.e., very wide RBFs) is undesirable because (i) the condition number of the interpolation matrix explodes as $(1/2)\exp(\pi^2/[4\alpha^2])$ [28] (ii) the RBF sum itself may be come very ill-conditioned [26] and (iii) the Runge Zone expands from the real interval $x \in [-1, 1]$ to the interior of the same rather large oval in the complex-plane as for polynomial interpolation [9]. On the other hand, saturation implies that the error will be disastrously huge when α is large or moderate. Like the Greek warrior-king Odysseus, who had to sail between the man-eating monster Scylla and the ship-eating ocean vortex Charybdis, RBF approximation has to navigate between two perils.

A useful pragmatic strategy is to therefore to choose the *largest* α compatible with the desired relative error tolerance δ where the word "relative" means that

$$\mathcal{E}/\|f\|_\infty \le \delta \tag{15}$$

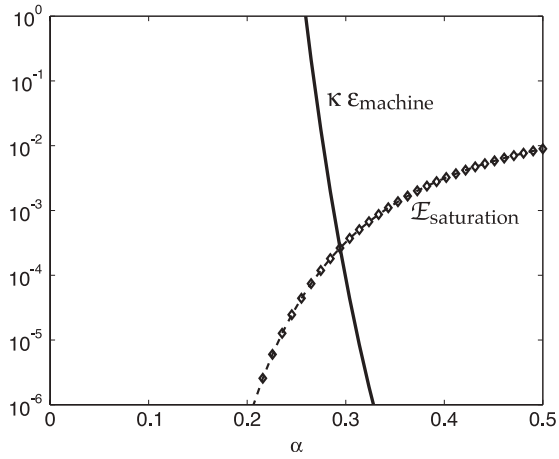

Fig. 7. The saturation error (dashed with circles) and the product of the condition number κ of the interpolation matrix with $\epsilon_{\text{machine}} = 2.2 \times 10^{-16}$.

where $\mathcal{E}$ is the absolute error in the L_∞ norm. Then we can avoid problems with error saturation by using the result found empirically above that

$$E_{\text{saturation}} \approx 0.058 \exp(-0.467/\alpha^2)\|f\|_\infty. \tag{16}$$

Solving the equation $E_{\text{saturation}}(\alpha)/\|f\|_\infty = \delta$ where $E_{\text{saturation}}$ is from (14) gives

$$\alpha_{\text{optimum}}(\delta) = \sqrt{\frac{0.5}{-\log(\delta/0.06)}} \tag{17}$$

where we have slightly rounded the floating point numbers in view of the uncertainties in the empirical saturation formula. This curve is graphed in Fig. 7 with α_{optimum} as the horizontal axis and δ (on a logarithmic scale) as the vertical axis.

We have shown above that the Runge Phenomenon is defeated by decreasing α sufficiently slowly with N. If we keep α fixed and take the limit, the Runge Phenomenon will be no difficulty as $N \to \infty$. However, the error will not converge to zero as $N \to \infty$, but only to our chosen tolerance δ.

Consequently, we cannot categorize this fixed-α strategy as an additional *convergent* strategy to defeat the Runge Phenomenon. However, in practice, the big trouble with either $\alpha \propto N^{-1/4}$ or $\alpha = \alpha_{\text{optimum}}(\delta)$ is that the needed α may be so small that the interpolation matrix may be horribly ill-conditioned. Fig. 7 shows that if δ is modest, say, 10^{-3}, one can choose $\alpha = 1/3$ and the matrix condition number is still small compared to the reciprocal of machine epsilon. However, demanding more accuracy — smaller δ — also requires smaller α, bringing us into the regime where $\kappa\epsilon_{\text{machine}} > 1$ and the solution of the interpolation matrix is badly compromised by the roundoff error. In the next section, we describe some partial remedies.

6. Strategies to fight the Ill-conditioning of the interpolation matrix

6.1. SVD factorization and filtering

The fastest way to compute the coefficients of the interpolant is by a Cholesky factorization of the interpolation matrix $\vec{\vec{G}}$. (Because $\vec{\vec{G}}$ is symmetric whenever the interpolation points and RBF centers coincide, this factorization in the form $\vec{\vec{G}} = \vec{\vec{L}}\vec{\vec{L}}^T$ is twice as fast as the usual LU factorization.) However, when the matrix is ill-conditioned, it is better to use the slower QR factorization, which suppresses roundoff by computing an orthogonal matrix as one of the factors, or by the slower but still more roundoff-suppressive SVD factorization:

$$\vec{\vec{G}} = \vec{\vec{U}}\vec{\vec{S}}\vec{\vec{V}}^T \tag{18}$$

where $\vec{\vec{S}}$ is a diagonal matrix whose elements σ_j, all real-valued and non-negative, are the "singular values" of the matrix $\vec{\vec{G}}$. Then $\vec{\vec{G}}\vec{\lambda} = \vec{f}$ is solved by

$$\vec{\lambda} = \vec{\vec{V}}\vec{\vec{S}}^{-1}\vec{\vec{U}}^T\vec{f}. \tag{19}$$

The usual matrix condition number κ is the ratio of the largest singular value to the smallest singular value. Any roundoff error in the part of $\vec{f}$ which projects onto the mode of the smallest singular value will be amplified, relative to the contribution

of the mode of the largest singular value, by $1/\kappa$. However, $\kappa\epsilon$ is truly the amplification of the roundoff error only in a worst-case situation; usually the modes of smallest singular value make only small contributions to the final answer. This allows a couple of tactics to find acceptable solutions to an ill-conditioned matrix.

First, modes of very small singular value, that is, σ_j such that

$$\sigma_j \le \sigma_{\text{cutoff}} \tag{20}$$

for some small, user-chosen σ_{cutoff} can be discarded by omitting the corresponding diagonal element from $\vec{\vec{S}}^{-1}$. This is equivalent to replacing $1/\sigma_j$ by zero in the diagonal matrix $\vec{\vec{S}}^{-1}$. Though it may sound rather bizarre to replace a very large number $1/\sigma_j$ by zero, this is a well-established procedure described in most linear algebra texts. The contributions of the corresponding columns of $\vec{\vec{U}}$ and $\vec{\vec{V}}$ to λ are likely to be controlled more by roundoff error than by reality because modes of small singular value are so enormously amplified. It is therefore usually beneficial to drop at least a few of the tiniest σ_j. "SVD filtering" is particularly useful in RBF Extension below.

6.2. Iterative correction

A simpler strategy to improve accuracy for an ill-conditioned matrix is "iterative correction". The first step is to define the matrix residua by substituting the solution back into the matrix problem that it is supposed to solve:

$$\vec{r} \equiv \vec{\vec{G}}\vec{\lambda} - \vec{f}. \tag{21}$$

If the matrix problem is well-conditioned, then $\vec{r}$ will be as small as machine precision, but for an ill-conditioned problem, $\vec{r}$ may have elements many orders of magnitude larger than machine epsilon. To compute the correction $\vec{\delta}$, solve the original problem with $\vec{r}$ replacing $\vec{f}$, that is,

$$\vec{\delta} = \vec{\vec{V}}\vec{\vec{S}}^{-1}\vec{\vec{U}}^T\vec{r} \tag{22}$$

where we have used the SVD form of the inverse of $\vec{\vec{G}}$. Then an improved approximation is

$$\vec{\lambda}^{(1)} = \vec{\lambda} - \vec{\delta}. \tag{23}$$

This procedure can be repeated until the correction ceases to diminish. Note that this is rather inexpensive because all factorizations of $\vec{\vec{G}}$, whether Cholesky, QR, or SVD, have costs proportional to N^3 whereas each iterative correction has a cost proportional to N^2.

Fig. 8 shows typical results. For very small α, iterative correction helps; for larger α when a simple LU or Cholesky factorization gives a moderately accurate answer, iterative correction *worsens* the error. Experiments with variations in σ_{cutoff} produced no improvement.

It is noteworthy that rather small values of α in the range of 1/10–1/20 were best for these exemplary functions. The interpolation matrix is *very* ill-conditioned for such small α, and Matlab printed nasty warning messages that the interpolation matrix was singular. Nevertheless, some accuracy was obtained.

6.3. Other Ill-conditioning strategies

Ill-conditioning is a major curse for RBF methods. We have described some simple but general strategies here. Other more RBF-specific schemes are reviewed in [21]. Kansa et al. [29,30] use an SVD-filtering scheme from [31]. Preconditioning strategies that accelerate iterative methods are widely used [32–37]. Yet another strategy is to change the RBF basis [38]. We make no claim that the methods for ill-conditioned RBF interpolation are the best, only that they were useful.

7. Defeating the Runge Phenomenon by RBF extension

One technique for defeating the Runge Phenomenon, and more generally, to apply the Fourier series to non-periodic problems, is "Fourier Extension". To approximate a function on a "physical interval", $x \in [-1, 1]$, the function $f(x)$ is approximated by an "extended function" $\tilde{f}(x)$ on a slightly larger interval, $x \in [-1 - D, 1 + D]$ where $D > 0$ is a small, positive constant. If $f(x)$ is known everywhere on the extended interval, this "Extension of the First Kind" in the terminology of [39] can be accomplished by multiplying the non-periodic function $f(x)$ by a "window" function to produce a modified function $\tilde{f}(x)$ which is periodic with period $(2 + 2D)$, but closely (or exactly) matches $f(x)$ on the "physical" interval.

If $f(x)$ is not explicitly known outside the physical interval, then one has a harder problem of "Extension of the Third Kind". Nevertheless, such extensions have been successfully made by a variety of authors as reviewed in [39,40]. Boyd and Ong [14] have shown that a Fourier Extension of the Third Kind is an exponentially-convergent method for approximating a non-periodic function $f(x)$ from knowledge only of samples of $f(x)$ on an evenly spaced grid of points.

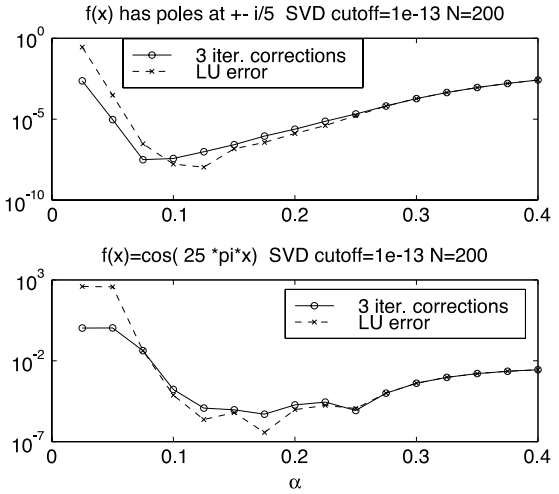

Fig. 8. Upper panel: $f(x) = 1/(1 + 25x^2) + 1/(1 + 25[x - 1]^2) + 1/(1 + 25[x + 1]^2)$ on $x \in [-1, 1]$. Lower panel: same but for $f(x) = \cos(25\pi x)$. $\sigma_{\text{cutoff}} = 10^{-13}$ for all computations.

The same strategy can be applied with radial basis functions. In this form of "Extension", a basis of Gaussian cardinal functions with *centers* evenly-spaced on the extended interval is used to approximate $f(x)$ on $[-1, 1]$ using interpolation points that are evenly spaced on the smaller, "physical interval", $[-1, 1]$.

Efficiency is greatly improved by exploiting parity. The symmetric and antisymmetric parts of $f(x)$ are

$$f_S(x) \equiv (1/2)\,(f(x) + f(-x))\,, \qquad f_A(x) \equiv (1/2)\,(f(x) - f(-x))\,. \tag{24}$$

Observe that by construction $f_S(-x) = f_S(x)$ and $f_A(-x) = -f_A(x)$. Because the approximation requires the factorization of a dense matrix at a cost of $O(N^3)$ floating point operations where N is the number of terms in the RBF approximation, it is cheaper by a factor of four to compute the approximations of $f_S(x)$ and $f_A(x)$ separately and then combine the results through

$$f(x) = f_S(x) + f_A(x). \tag{25}$$

To compute $f_S(x)$, use the centers

$$x_j^c \equiv j(1 + D)/N_{\text{sym}}, \quad j = 0, 1, \ldots, N_{\text{sym}} \tag{26}$$

where $N_{\text{sym}} + 1$ is the number of non-negative centers. Expand

$$f_S \approx \sum_{j=0}^{N_{\text{sym}}} \lambda_j \phi_j(x) \tag{27}$$

with the symmetrized basis functions

$$\phi_j(x) \equiv \left\{\exp\left(-[\alpha^2/h^2](x - x_j)^2\right) + \exp\left(-[\alpha^2/h^2](x + x_j)^2\right)\right\}. \tag{28}$$

Let the elements of a vector $\vec{f}$ be

$$f_i = f(x_i), \quad i = 1, \ldots, N_{\text{coll}} \tag{29}$$

where N_{coll} is the number of collocation points. Define the rectangular matrix $\vec{\vec{G}}$ to have the elements

$$G_{ij} \equiv \phi_{j-1}(x_i), \quad i = 1, \ldots, N_{\text{col}},\ j = 1, 2, \ldots, N_{\text{sym}+1}. \tag{30}$$

Let $\vec{\lambda}$ store the coefficients of the RBF series. Then $\vec{\lambda}$ solves the matrix equation

$$\vec{\vec{G}}\vec{\lambda} = \vec{f}. \tag{31}$$

When the number of collocation points is equal to the number of spectral coefficients λ_j, the matrix $\vec{\vec{G}}$ is square and the matrix problem can be solved — but not well — by ordinary LU factorization. Unfortunately, the extension of a function is inherently ill-posed as explained in [39]. Therefore, we used an SVD factorization of the interpolation matrix with three additional tricks:

1. SVD cutoff
2. overdetermination
3. iterative correction.

The first and last were explained in the previous section.

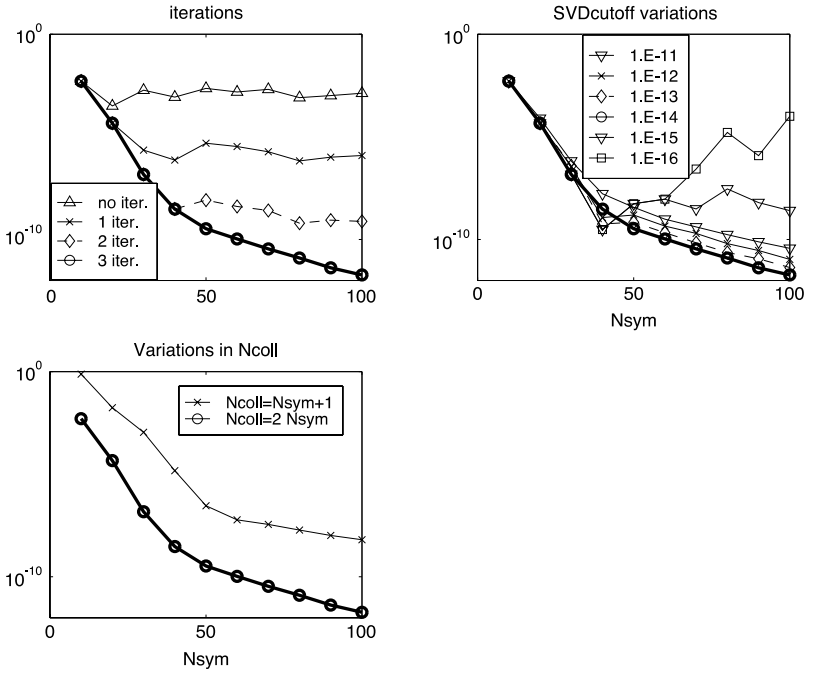

Fig. 9. RBF Extension for the six-pole Runge function, $f(x) = 1/(1 + 25x^2) + 1/(1 + 25[x - 1]^2) + 1/(1 + 25[x + 1]^2)$ with $\alpha = 0.5$ and an extended interval of $x \in [-1.1, 1.1]$ (that is, $D = 1/10$). The thick curve in each graph shows the maximum pointwise error on the physical interval, $x \in [-1, 1]$, of the default case; this used three iterative corrections, twice as many collocation points $N_{\rm coll}$ as the degree of the approximation N and discarded singular values smaller than an SVD cutoff of 10^{-14}. Upper left: maximum pointwise error, when three, two, one and zero iterative corrections are used. Upper right: effects of varying the cutoff in singular values (with three iterative corrections). Lower left: the upper curve is the error in interpolation.

If $N_{\rm coll} > N_{\rm sym} + 1$, the interpolation matrix $\vec{\vec{G}}$ is rectangular instead of square and the overdetermined interpolation problem has no solution. However, the SVD formula (22) generates a least-squares approximation to the overdetermined problem. As explained in [39] for Fourier Extension, it is advantageous to take

$$N_{\rm coll} = 2N. \tag{32}$$

The reason is that using more collocation points than spectral coefficients constrains the extended function more strongly than pure interpolation, and reduces the inherent ill-conditioning.

Fig. 9 shows the effects of iterative correction, described in the previous section, for the RBF extension of a typical $f(x)$. This was chosen to be the sum of Runge's function plus two translated copies of the function so that there are six poles in $f(x)$ at $x = \pm i/5, \pm 1 \pm i/5$. In all three panels, the default choice of numerical parameters is the thick curve with circles, which employed $\sigma_{\rm cutoff} = 10^{-14}$, $N_{\rm coll} = 2N_{\rm sym}$, an extended interval 10% wider than the physical interval, and three iterative corrections. This choice of parameters yields a maximum pointwise error (on the physical interval where all the collocation points lie) is about 10^{-12} with one hundred symmetrized RBF!

The upper left graph shows that the error plateaus at a rather large error without iterative correction. Because each correction is very cheap compared to the SVD factorization, it is highly recommended.

The upper right panel shows that using a very small cutoff $\sigma_{\rm cutoff}$, which is equivalent to keeping all the SVD modes, forces the error to rise, instead of fall, with $N_{\rm sym}$. Any choice of cutoff in the rather large range 10^{-14}–10^{-11} gave rapid convergence with N.

The lower panel shows that — with iterative corrections and SVD filtering — RBF Extension converges even for interpolation with the number of collocation points equal to the number of basis functions. However, the rate of convergence and the error are both dramatically improved by oversampling.

Fig. 10 answers the question: Is RBF Extension useful? The figure shows that the unextended approximation is fairly accurate with the SVD filtering/over-collocation/iterative correction tricks. However, the convergence ceases for rather small values of $N_{\rm sym}$ at a minimum of error which is many orders of magnitude larger for the unextended problem than for RBF Extension.

Other obvious questions are: how does RBF Extension cope with singularities closer to the real axis? How sensitive is the method to the width of the extension region? Using an exemplary function with singularities at $\pm i/20$ near $x = 0, \pm 1$, the contour plot of errors in Fig. 11 answers both questions. As the singularities move closer to the real axis, one needs larger N, but it is still possible to obtain high accuracy, in this case at least nine decimal places. The contours are nearly vertical, implying that the error is very insensitive to D and depends almost entirely on N. The roughly linear spacing of the

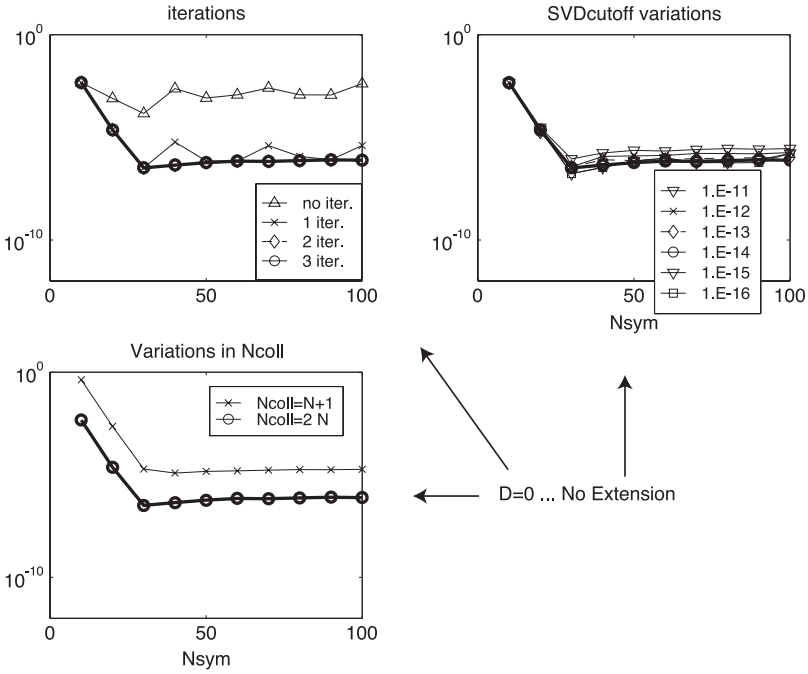

Fig. 10. Same as the previous figure but with $D = 0$. This means there is no extension.

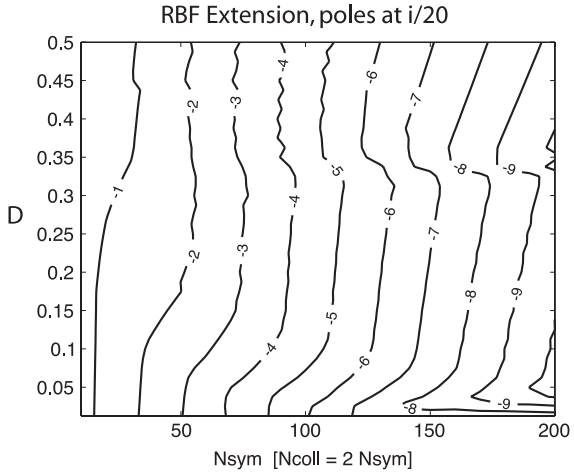

Fig. 11. RBF Extension: base-10 logarithm of the L_∞ errors for $f(x) = 1/(1 + 400x^2) + 1/(1 + 400[x - 1]^2) + 1/(1 + 400[x + 1]^2)$ on $x \in [-1, 1]$. The vertical axis D is the size of the unphysical extension subintervals. Note that an overdetermined system was solved so that the approximation used twice as many samples of $f(x)$ as the number of RBFs. All singular values smaller than 10^{-12} were removed. The RBF inverse width $\alpha = 1/2$. Symmetry was exploited by approximating the symmetric part of $f(x)$ — in this case, there is no antisymmetric part — on $x \in [0, 1]$. Thus, the results for $N_{\text{sym}} = 200$ actually require a total of 800 grid point values of $f(x)$ on $[-1, 1]$.

contours of the logarithm of the error shows that the error falls geometrically with N, as seen also in the line graphs in the two previous figures.

8. Three-interval method

8.1. Windowing and the middle subinterval

Windowing is a common trick in time series analysis: a long, nonperiodic, non-decaying time series is multiplied by a "window" function that is a smoothed top hat function, that is, a function that is approximately one over an interval of finite width and then decays smoothly and exponentially to zero for larger times. The windowed function, because it is zero for both large and small times, can be approximated well by a Fourier series or transform and analyzed for periodicities, such as accurately computing the annual cycle in a hundred-year time series of weather data.

The same trick can be applied to a function $f(x)$ to convert a finite interval approximation problem into an infinite interval approximation problem. A suitable window (from a myriad of possibilities) is

$$\mathcal{T}(x;\Omega,b) \equiv (1/2)\{\mathrm{erf}(\Omega(x+b)) - \mathrm{erf}(\Omega(x-b))\} \tag{33}$$

where Ω ("inverse width") and b ("breadth") are positive constants. If $\Omega \gg 1$, as in applications, then

$$\mathcal{T}(x;\Omega,b) \approx \begin{cases} 1, & x \in [-b,b] \\ 0, & |x| > b \end{cases} \qquad \Omega \gg 1. \tag{34}$$

If b is a little less than one, then the windowed function

$$f_{\mathrm{center}}(x;\Omega,b) \equiv f(x)\mathcal{T}(x;\Omega,b) \tag{35}$$

has negligible amplitude for $|x| > 1$. It follows that we can expand $f_{\mathrm{center}}(x)$ on an infinite interval using only centers and interpolation points on the truncated interval $x \in [-1, 1]$. The Runge Phenomenon is impossible for an infinite interval expansion and thus for $f_{\mathrm{center}}(x)$.

The parameter Ω can be chosen only moderately large because in the limit $\Omega \to \infty$, $\mathcal{T}$ is a pair of step-functions, discontinuous at $x = \pm b$. The discontinuities in $\mathcal{T}$ are passed on to the function $f_{\mathrm{center}}(x)$, which therefore has an RBF series that converges very slowly. For moderately large Ω and b a little smaller than one, it is possible to obtain a windowed function $f_{\mathrm{center}}(x)$ that has an exponentially-convergent RBF expansion, no Runge Phenomenon, and still approximates $f(x)$ well over *most* of the interval $x \in [-1, 1]$.

8.2. Boundary layers: the outer subintervals

Unfortunately, there are "boundary layers" (to borrow a term from fluid mechanics) near $x = \pm 1$ where $f_{\mathrm{center}}(x)$ is, because of the rapid decay of the window function factor, a poor approximation to $f(x)$. This is easily fixed by using a finite interval expansion not for the whole domain, but only on the *small* interval $x \in [-1, -1 + 2D]$ and similarly in the right boundary layer where

$$D = 1 - b. \tag{36}$$

This would seem to be a circular argument because the goal of introducing the windowed function f_{center} was to avoid a finite interval expansion and the possibility of the Runge Phenomenon, and yet here we suggest using exactly such a dangerous finite interval expansion in the boundary layers!

There are two options: a "contracting-layer" strategy and a small-but-fixed D strategy. The "contracting-layer" scheme was introduced by Boyd for polynomial approximation in [13]: choose D proportional to $1/\sqrt{N}$ or some other negative power so that the width of the boundary layer *shrinks* with increasing N. It is shown in that note, using a Fourier series for f_{center} and an ordinary Lagrangian polynomial interpolation for the boundary layers, that this three-interval approach is (i) free of the Runge Phenomenon and (ii) converges at an exponential but subgeometric rate. This convergence is rigorously proved for polynomial interpolation in [15]. Although we shall not offer a formal proof here, the numerical results show that the same is true for the three-interval RBF strategy described here.

The second approach is to simply use a small, fixed boundary layer width D with the caveat that it may be necessary to retreat and try again with smaller D if the first choice gives divergence with increasing N. The justification for the "fixed-width" strategy is that Platte and Driscoll [9] showed that the Runge Zone $\mathcal{D}(\beta)$ for RBF interpolation with uniformly-spaced points and centers is always smaller than that for polynomial interpolation. Furthermore, it is known that for polynomial interpolation, the Runge Zone extends to at most a distance of 0.5255 from the canonical interval $x \in [-1, 1]$. This (and a trivial rescaling from $[-1, 1]$ to our boundary layers of width $2D$) proves the following:

Theorem 1. *If $f(x)$ is free of singularities everywhere within a distance ϵ of the interval $x \in [-1, 1]$, then the three-interval RBF method is guaranteed to converge as long as D, the half-width of the boundary layers (which are each of length $2D$) satisfy the inequality*

$$D < \epsilon/0.5255. \tag{37}$$

Fixed D guarantees a geometric rate of convergence — a slow geometric rate if D is small but nonetheless a geometric rate — as $N \to \infty$.

8.3. Summary of the algorithm

$$f_{\text{three-interval}} = \begin{cases} f_{\mathrm{left},M}, & x \in [-1, -1+2D] \\ f_{\mathrm{center},N}, & x \in [-1+2D, 1-2D] \\ f_{\mathrm{right},M}, & x \in [1-2D, 1] \end{cases} \tag{38}$$

where the number of degrees of freedom in each boundary layer is M and $f_{\text{center},N}$ is determined by the $(N+1)$ interpolation conditions

$$f_{\text{center},N}(x_j) = f(x_j)\mathcal{T}(x_j;\, \Omega, b) \tag{39}$$

while $f_{\text{left},M}$ satisfies the interpolation conditions

$$f_{\text{left},M}(x_j) = f(x_j), \quad j = 1, 2, \ldots, M+1 \tag{40}$$

and similarly

$$f_{\text{right},M}(x_j) = f(x_j), \quad j = N-M, \ldots, N+1 \tag{41}$$

where, for all three subintervals, the centers of the RBFs coincide with the interpolation points, and the number of RBFs in each of the three series is equal in number to the interpolation points/centers for that subproblem. Note that only the forcing for the center problem is windowed; the boundary layer subproblems is the original $f(x)$. Although $f_{\text{center},N}(x)$ solves an interpolation problem on the entirety of $x \in [-1, 1]$, it is summed, to graph $f(x)$, only on the middle interval where it is a good approximation to $f(x)$.

8.4. Numerical parameters

One disadvantage of the three-interval RBF method is that it lives in a three-dimensional parameter space (α, D, Ω) whereas the standard single-interval RBF method has only a one-dimensional parameter space (α). Fortunately, numerical accuracy for any given $f(x)$ varies analytically and therefore smoothly with α, D and Ω.

The Greek proverb "moderation in all things" applies to choosing these three parameters:

1. The inverse width of the RBFs, α, must not be too small because the condition number grows as $O(\exp(\pi^2/(4\alpha^2)))$ as $\alpha \to 0$.
2. However, α must be small compared to one, or otherwise the error will plateau with N at $E_{\text{saturation}} \approx 0.058\exp(-0.467/\alpha^2)$ as demonstrated as (14) of Section 4.
3. Thus, α should be chosen somewhere in the range 1/10–1/5 so as to steer a middle course between an error saturation, which is proportional to $\exp(-0.467/\alpha^2)$ and the condition number of the interpolation matrix, which is proportional to $\exp\left([\pi^2/4]/\alpha^2\right)$.
4. The oscillations seen in Fig. 1 are reduced from $O(f(\pm 1))$ to $O(\mathcal{T}(\pm 1)f(\pm 1))$ by windowing. It follows that windowing is only effective if
$$\mathcal{T}(\pm 1;\, \Omega, 1-D) \ll 1 \leftrightarrow \Omega D \gg 1. \tag{42}$$
5. D must be smaller than 1/2 because otherwise the boundary layers, each of length $2D$, fill the entire interval, leaving no room for a center interval! Indeed, D must be small compared to 1/2 so that the boundary layers are thin, justifying their name, and allowing the three-interval method to satisfy (37) and converge even when $f(x)$ has singularities close to the interval $x \in [-1, 1]$.
6. The smallness of D implies that Ω must be moderately large, typically at least ten. However, Ω cannot be huge because then the window is a sum of step functions, $f_{\text{center}}(x)$ is discontinuous at $x = \pm(1-D)$, and its RBF series displays the same Gibbs' oscillations evident in Fig. 1.

Fig. 12 shows some typical results.

9. Summary and comparison of successful methods

In this work, we have tried to add several tiles to the mosaic of the theory of radial basis functions, concentrating on Gaussian RBFs on a finite interval. The most interesting applications of RBFs are on *irregular* grids, but it is obviously important to understand the strengths and weaknesses of a method on a uniform grid before attacking the more complex task of adaptive, variable grid applications.

We discussed several strategies for defeating the Runge Phenomenon. Using a basis of infinite interval cardinal functions failed due to the Gibbs Phenomenon near the endpoints of the finite interval. Replacing just the *interior* cardinal functions with their infinite interval counterparts was an even bigger fiasco. A smooth blend of finite and infinite interval cardinal functions was a flop as well. There are three strategies that worked.

The three effective RBF strategies have such wide differences in cost, complexity and achievable accuracy that comparing them is a little like comparing ballet, disco and the waltz. Nevertheless, Table 1 catalogues their qualitative properties while the errors are compared in Table 2.

The first good strategy is to vary α with the number of interpolation points N as $N^{-1/4}$. This seems to always succeed in giving a *subgeometric* rate of convergence for the approximation (error falling as $\exp(-q\sqrt{N})$ for some constant q). Unfortunately, the matrix condition number grows as $\exp(p\sqrt{N})$ for some $p > 0$. In many applications, though, this strategy of α decreasing as $N^{-1/4}$ would be successful in generating highly accurate approximations from knowledge of $f(x)$ only on an equispaced grid.

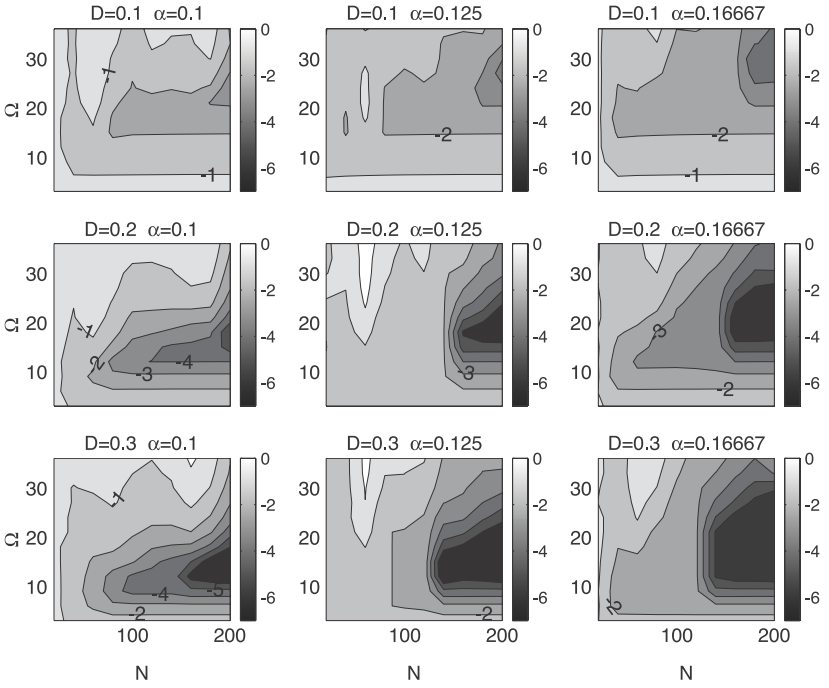

Fig. 12. Three-interval RBF: base-10 logarithm of the maximum pointwise error for $f(x) = 1/(1+25x^2) + 1/(1+25[x-1]^2) + 1/(1+25[x+1]^2)$, same as in the previous figures. The various half-thicknesses of the boundary layer D and various RBF inverse widths α as marked in the title of each subplot. The vertical axis is Ω, the reciprocal of the width of the smoothing zones in the window function, $\mathcal{T}(x;\Omega,b) \equiv (1/2)\{\mathrm{erf}(\Omega(x+b)) - \mathrm{erf}(\Omega(x-b))\}$, used to compute the approximation on the central interval.

Table 1
Features of good RBF methods.

Property	α-decrease	RBF extension	Three-interval
Parameters	One: α	Three: α, D, σ_{cutoff}	Three: α, D, Ω
Oversampling?	No	Recommended	No
Simplicity	Best	Worst	Moderate
Matrix method	LU[a]	SVD	LU[a]

[a] For small α, LU may need iterative correction and/or replacement by SVD with filtering.

Table 2
Errors of optimized RBF methods for $N = 200$.

Strategy → $f(x)$ ↓	α-decrease	Exten. $N = 200$	Exten. $N_{\mathrm{coll}} = 200$	3-interval
$\cos(25\pi x)$	3.7E−7	1.7E−12	1.3E−8	2.1E−6
$\cos((100/3)\pi x)$	6.7E−6	1.4E−11	2.0E−4	2.9E−5
$\cos(50\pi x)$	9.4E−4	3.0E−9	1.15	2.7E−2
$\rho = 25$	6.4E−9	1.3E−13	5.8E−9	1.30E−8
$\rho = 400$	8.37E−6	3.5E−5	1.8E−2	1.7E−3

A noncovergent-but-practical strategy is to choose an error tolerance δ and then fix α at the *largest* RBF width parameter whose saturation error is less than or equal to δ: $\alpha = \alpha_{\mathrm{optimum}}(\delta) = \sqrt{0.5/[-\log(\delta/0.06)]}$. One then increases N until the error saturates at $\max_{x\in[-1,1]} |f(x) - f_N(x;\alpha) \approx \delta$. Note that because of the phenomenon of error saturation, the error can be reduced further (below δ) only by decreasing α, even if N is a trillion.

The second convergent strategy is RBF Extension. Although much more expensive because it requires an SVD factorization, and (usually) over-collocation with more sample points than degrees-of-freedom, RBF Extension is more resistant to the ill-conditioning, achieving much greater accuracy than the "α-decrease" method.

The third good strategy is to use three subintervals. This was the least accurate of the three successful strategies.

Standard interpolation with "α-decrease" (or fixed $\alpha_{\mathrm{optimum}}(\delta)$) is our recommended strategy whenever satisfactory accuracy can be obtained before ill-conditioning intervenes. The RBF Extension Method is the worst in both simplicity and cost, but has the not-inconsiderable virtue of generating much smaller errors than the alternatives, that is, of better fighting the ill-conditioning that is both the spoor of the Runge Phenomenon and also an inherent difficulty of RBFs with small α.

Although all our examples employed a uniform grid, all these successful strategies can be applied to highly irregular, adaptive grids. But that is a tale for another article.

Acknowledgements

This work was supported by NSF Grants OCE998636, OCE0451951 and ATM 0723440.

References

[1] M.D. Buhmann, Radial Basis Functions: Theory and Implementations, in: Cambridge Monographs on Applied and Computational Mathematics, vol. 12, Cambridge University Press, 2003.
[2] H. Wendland, Scattered Data Approximation, Cambridge University Press, 2005.
[3] M.D. Buhmann, Radial basis functions, Acta Numer. 9 (2000) 1–38.
[4] R. Schaback, H. Wendland, Kernel techniques: from machine learning to meshless methods, Acta Numer. 15 (2006) 543–639.
[5] G.E. Fasshauer, Newton iteration with multiquadrics for the solution of nonlinear PDEs, Comput. Math. Appl. 43 (2002) 423–438.
[6] P.P. Chinchapatnam, K. Djidjeli, P.B. Nair, Unsymmetric and symmetric meshless schemes for the unsteady convection–diffusion equation, Comput. Methods Appl. Mech. Engrg. 195 (2006) 2432–2453.
[7] A.I. Fedoseyev, M.J. Friedman, E.J. Kansa, Continuation for nonlinear elliptic partial differential equations discretized by the multiquadric method, Internat. J. Bifur. Chaos 10 (2000) 481–492.
[8] A.I. Fedoseyev, M.J. Friedman, E.J. Kansa, Improved multiquadric method for elliptic partial differential equations via PDE collocation on the boundary, Comput. Math. 43 (2002) 439–455.
[9] R.B. Platte, T.A. Driscoll, Polynomials and potential theory for Gaussian radial basis function interpolation, SIAM J. Numer. Anal. 43 (2005) 750–766.
[10] B. Fornberg, J. Zuev, The Runge Phenomenon and spatially variable shape parameters in RBF interpolation, Comput. Math. Appl. 54 (2007) 379–398.
[11] J.P. Boyd, F. Xu, Divergence (Runge Phenomenon) for least-squares polynomial approximation on an equispaced grid grid and Mock–Chebyshev subset interpolation, Appl. Math. Comput. 210 (2009) 158–168.
[12] J.P. Boyd, Defeating the Runge Phenomenon for equispaced polynomial interpolation via Tikhonov regularization, Appl. Math. Lett. 5 (1992) 57–59.
[13] J.P. Boyd, Exponentially accurate Runge-free approximation of non-periodic functions from samples on an evenly-spaced grid, Appl. Math. Lett. 188 (2007) 1780–1789.
[14] J.P. Boyd, J.R. Ong, Exponentially-convergent strategies for defeating the Runge Phenomenon for the approximation of non-periodic functions, part I: single-interval schemes, Commun. Comput. Phys. 5 (2009) 484–497.
[15] J.P. Boyd, J.R. Ong, Exponentially-convergent strategies for defeating the Runge Phenomenon for the approximation of non-periodic functions, part II: multi-interval schemes, Appl. Numer. Math. (2009) (submitted for publication).
[16] B. Fornberg, N. Flyer, Accuracy of radial basis function interpolation and derivative approximations on 1-D infinite grids, Adv. Comput. Math. 23 (2005) 5–20.
[17] J.P. Boyd, L. Wang, Truncated Gaussian RBF differences are always inferior to finite differences of the same stencil width, Commun. Comput. Phys. 5 (2009) 42–60.
[18] J.P. Boyd, L. Wang, An analytic approximation to the cardinal functions of Gaussian radial basis functions on a one-dimensional infinite uniform lattice, Appl. Math. Comput. 215 (2009) 2215–2223.
[19] J.P. Boyd, L. Wang, Asymptotic coefficients for Gaussian radial basis function interpolants, Appl. Math. Comput. 216 (2010) 2394–2407.
[20] J.P. Boyd, L. Wang, A Fourier error analysis for Gaussian radial basis functions on an infinite uniform grid, Commun. Comput. Phys. (2011) (in press).
[21] G.F. Fasshauer, Meshfree Approximation Methods with MATLAB, in: Interdisciplinary Mathematical Sciences, World Scientific Publishing Company, Singapore, 2007.
[22] T.A. Driscoll, A. Heryudono, Adaptive residual subsampling methods for radial basis function interpolation and collocation problems, Comput. Math. Appl. 53 (2007) 927–939.
[23] J.P. Boyd, Chebyshev and Fourier Spectral Methods, 2nd ed., Dover, Mineola, New York, 2001, 665 pp.
[24] L.N. Trefethen, D. Bau III, Numerical Linear Algebra, Society for Industrial and Applied Mathematics (SIAM), Philadelphia, 1997.
[25] V. Maz'ya, G. Schmidt, On approximate approximation using Gaussian kernels, IMA J. Numer. Anal. 16 (1996) 13–29.
[26] J.P. Boyd, L.R. Bridge, Sensitivity of RBF interpolation on an otherwise uniform grid with a point omitted or slightly shifted, Appl. Numer. Math. 60 (2010) 659–672.
[27] J.P. Boyd, Error saturation in Gaussian radial basis functions on a finite interval, J. Comput. Appl. Math. 234 (2010) 1435–1441.
[28] J.P. Boyd, K.W. Gildersleeve, Numerical experiments on the condition number of the interpolation matrices for radial basis functions, Appl. Math. Comput. (2009) (submitted for publication).
[29] A. Emdadi, E.J. Kansa, N.A. Libre, M. Rahimian, M. Shekarchi, Stable PDE solution methods for large multiquadric shape parameters, CMES Comput. Model. Eng. Sci. 25 (2008) 23–41.
[30] N.A. Libre, A. Emdadi, E.J. Kansa, M. Rahimian, M. Shekarchi, A stabilized RBF collocation scheme for Neumann type boundary value problems, CMES Comput. Model. Eng. Sci. 24 (2008) 61–80.
[31] K.Y. Volokh, O. Vilnay, Pin-pointing solution of ill-conditioned square systems of linear equations, Appl. Math. Lett. 13 (2000) 119–124.
[32] D. Brown, L. Ling, E. Kansa, J. Levesley, On approximate cardinal preconditioning methods for solving PDEs with radial basis functions, Eng. Anal. Bound. Elem. 29 (2005) 343–353.
[33] N. Dyn, D. Levin, S. Rippa, Numerical procedures for surface fitting of scattered data by radial functions, SIAM J. Sci. Comput. 7 (1986) 639–659.
[34] L.V. Ling, E.J. Kansa, Preconditioning for radial basis functions with domain decomposition methods, Math. Comput. Modelling 40 (2004) 1413–1427.
[35] L.V. Ling, E.J. Kansa, A least-squares preconditioner for radial basis functions collocation methods, Adv. Comput. Math. 23 (2005) 31–54.
[36] R. Schaback, Multivariate interpolation by polynomials and radial basis functions, Constr. Approx. 21 (2005) 293–317.
[37] R. Schaback, Limit problems for interpolation by analytic radial basis functions, J. Comput. Appl. Math. 212 (2008) 127–149.
[38] B. Fornberg, C. Piret, A stable algorithm for flat radial basis functions on a sphere, SIAM J. Sci. Comput. 30 (2007) 60–80.
[39] J.P. Boyd, A comparison of numerical algorithms for Fourier extension of the first, second and third kinds, J. Comput. Phys. 178 (2002) 118–160.
[40] J.P. Boyd, Fourier embedded domain methods: extending a function defined on an irregular region to a rectangle so that the extension is spatially periodic and C^∞, Appl. Math. Comput. 161 (2005) 591–597.